In any case, the present data clearly suggest that even larger cations of this same type with the general formula $[R_2B(\mu\text{-}pz)_2\{B(\mu\text{-}pz)_2\}_nBR_2]^{n+}$ should be accessible; terminal R substituents of a structural unit $(\mu\text{-}pz)_2BR_2$ have been replaced by halogen,[12,14] which, in turn, was replaced by pyrazolyl groups,[13] thus providing a site for further chain elongation.

Acknowledgment. This work was supported by the Office of Naval Research (K.N.). Dr. J. Bielawski developed the synthesis of $[(C_2H_5)_2B(\mu\text{-}pz)_2B(\mu\text{-}pz)_2B(C_2H_5)_2]^+PF_6^-$ originating from $K[B(pz)_4]$; W. J. Layton recorded the NMR spectra.

Registry No. $[H_2B(\mu\text{-}pz)_2B(\mu\text{-}pz)_2BH_2]^+PF_6^-$, 97073-75-1; $[H_2B(\mu\text{-}pz)_2B(\mu\text{-}pz)_2B(C_2H_5)_2]^+PF_6^-$, 97073-77-3; $[(C_2H_5)_2B(\mu\text{-}pz)_2B(\mu\text{-}pz)_2B(C_2H_5)_2]^+PF_6^-$, 40249-67-0; $[H_2B(\mu\text{-}pz)_2B(\mu\text{-}pz)_2B(\mu\text{-}pz)_2BH_2]^{2+}[PF_6^-]_2$, 97102-13-1; $[(C_2H_5)_2B(\mu\text{-}pz)_2B(\mu\text{-}pz)_2B(\mu\text{-}pz)_2B(C_2H_5)_2]^{2+}[PF_6^-]_2$, 40249-68-1; $(CH_3)_3N{\cdot}BH_2I$, 25741-81-5; $(pz)_2B(\mu\text{-}pz)_2BH_2$, 92242-00-7; $(C_2H_5)_2BOts$, 97073-78-4; $(C_2H_5)_2B(\mu\text{-}pz)_2B(pz)_2$, 86050-17-1; $[(pz)_4B]^-K^+$, 14782-58-2; $(pz)_2B(\mu\text{-}pz)_2B(pz)_2$, 16243-58-6.

(14) Hanecker, E.; Hodgkins, T. G.; Niedenzu, K.; Nöth, H. *Inorg. Chem.* **1985**, *24*, 459.

Contribution from the Department of Chemistry, University of California, Davis, California 95616

Proton Nuclear Magnetic Resonance Studies of Iron Porphyrin Complexes with a Vinyl Carbene Inserted between Iron and a Pyrrole Nitrogen

ALAN L. BALCH,* RU-JEN CHENG, GERD N. LA MAR,* and LECHOSLAW LATOS-GRAZYNSKI

Received February 15, 1985

Proton NMR spectra have been obtained for the paramagnetic ($S = {}^3/_2$) iron(III) complexes P[C=C(*p*-$C_6H_4Cl)_2$]FeX (X = Cl, Br, I; P = porphyrin dianion from *meso*-tetraarylporphyrin, or protoporphyrin IX dimethyl ester). Functional group assignments have been made with use of selective deuterium and methyl labeling. More detailed assignments have been made on the basis of the temperature dependence of the spectra and analysis of the line widths, which are dominated by dipolar relaxation. The spectra are indicative of C_s symmetry for these complexes in solution. This result is in accord with the solid-state structure of these complexes but requires some oscillatory motion of one of the *p*-ClC_6H_4 groups. The dominant π-spin transfer to the pyrroles indicates that, of the alternate ground states $(d_{xy})^2(d_{xz})^1(d_{yz})^1(d_{x^2-y^2})^1$ and $(d_{xy})^2(d_{xz})^1(d_{yz})^1(d_{z^2})^1$, the latter is present. The complexes exhibit axial magnetic anisotropy dominated by negative zero-field splitting. For the protoporphyrin IX derivative, the spectrum indicates that the four isomers resulting from carbene insertion into each of the four distinct Fe–N bonds are present.

Introduction

Recently several remarkable reactions of metalloporphyrins that involve the transfer of substituents from metal to pyrrole nitrogen have been discovered.[1-10] The carbene migration shown in eq 1 is an example in which the migration is coupled with a redox reaction.[3-5] The process is reversible.

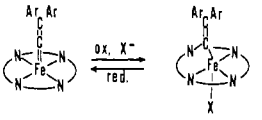

1 2 (1)

The formation of **2** via reaction 1 has produced several suggestions regarding the nature of highly oxidized forms of heme proteins which are involved in the mechanism of action of the peroxidases and cytochromes P450. Thus a species analogous to **2** but with an oxygen atom replacing the carbene moiety has been considered as a structural alternative to the more conventional iron oxo unit in highly oxidized heme proteins.[3,4] Spectroscopic similarities between **2** and the enzymic intermediate, catalase compound I, have produced the proposal that similar structures are involved.[3] It has been suggested that an oxygen atom migration analogous to reaction 1 might be involved in heme degradation that is produced by heme oxygenase.[4,9]

The insertion product **2** has been characterized by two independent X-ray diffraction studies.[3,9] Magnetic susceptibility, electron spin resonance, and Mössbauer spectroscopic studies indicate that this complex is best described as an iron(III) complex with an $S = {}^3/_2$ ground state.[5]

Proton NMR spectroscopy provides a uniquely useful probe for studying the structure of iron porphyrins in solution.[11] For paramagnetic complexes the hyperfine shift patterns are particularly sensitive to the spin, ligation, and oxidation state of the metal. For complexes derived from synthetic, symmetric porphyrins, the presence of a substituent on one nitrogen reduces the symmetry to at most C_s and thereby introduces a greater inherent complexity to their NMR spectra. Here we report a detailed examination of the ^1H NMR spectra of a variety of substituted forms of **2**.

Results and Discussion

Assignment of ^1H NMR Resonances to Functional Groups through Labeling Studies. Our analysis of the complex spectra of **2** and variously substituted derivatives relates directly to the geometric information available from the X-ray studies. The structure of **2** as determined by X-ray diffraction[9] is shown in Figure 1. While the molecule has no symmetry in the solid state, it appears to have C_s symmetry in solution, with the mirror plane passing through the iron atom, the axial chloride ligand, and the carbene carbon. Accordingly, labels have been affixed to the four pyrrole (pyrr) positions and to the four phenyl rings.

The full ^1H NMR spectrum of **2** (X = I; C, D = *p*-C_6H_5) in chloroform-*d* solution is shown in Figure 2. Four resonances, three upfield and one downfield, are particularly evident. On the

(1) Ogoshi, H.; Omura, T.; Yoshida, Z. *J. Am. Chem. Soc.* **1973**, *95*, 1666.
(2) Ogoshi, H.; Watanabe, E.; Koketzu, N.; Yoshida, A. *J. Chem. Soc., Chem. Commun.* **1974**, 943.
(3) Chevrier, B.; Weiss, R.; Lauge, M.; Mansuey, D.; Chottard, J. C. *J. Am. Chem. Soc.* **1981**, *103*, 2899.
(4) Latos-Grazynski, L.; Cheng, R.-J.; La Mar, G. N.; Balch, A. L. *J. Am. Chem. Soc.* **1981**, *103*, 4270.
(5) Mansuy, D.; Morgenstern-Badarau, I.; Lange, M.; Gaus, P. *Inorg. Chem.* **1982**, *21*, 1427.
(6) Dolphin, D.; Halko, D. J.; Johnson, E. *Inorg. Chem.* **1981**, *20*, 4348.
(7) Mansuy, D.; Battioni, J.-P.; Dupré, D.; Satori, E.; Chottard, G. *J. Am. Chem. Soc.* **1982**, *104*, 6159.
(8) Ortiz de Montellano, P. R.; Kunze, K. L.; Augusto, O. *J. Am. Chem. Soc.* **1982**, *104*, 3545.
(9) Olmstead, M. M.; Cheng, R.-J.; Balch, A. L. *Inorg. Chem.* **1982**, *21*, 4143.
(10) Lancon, D.; Cocolios, P.; Guilard, R.; Kadish, K. M. *J. Am. Chem. Soc.* **1984**, *106*, 4472.
(11) La Mar, G. N.; Walker (Jensen), F. A. In "The Porphyrins"; Dolphin, D., Ed.; Academic Press: New York, 1979; Vol. 4, p 61.

0020-1669/85/1324-2651$01.50/0

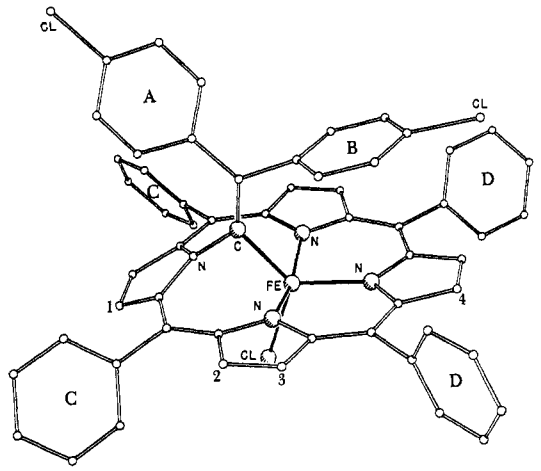

Figure 1. Drawing of the solid-state structure of **2** adapted from the X-ray crystallographic study.[9] Within the labeling scheme shown, ortho and meta protons on the equivalent pair of rings D will be labeled O_D and M_D respectively and other protons will be designated similarly.

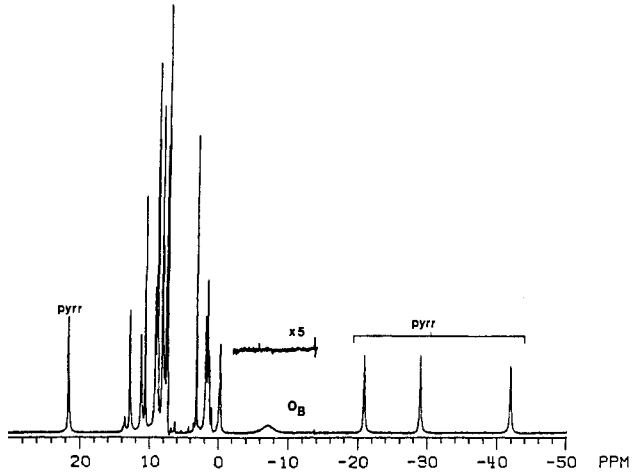

Figure 2. 360-MHz ^{1}H NMR spectrum of **2** (X = I; C, D = C_6H_5) in chloroform-*d* solution at 25 °C. Peaks labeled pyrr are due to the pyrrole protons. The inset shows a part of the spectrum of deuterated **2** (X = I; C, D = C_6H_5; Ar = *p*-C_6D_4Cl).

basis of deuterium-labeling studies these have been assigned to the four pyrrole protons that are present in the structure as seen in Figure 1. These four prominent resonances remain at full intensity in samples of **2** that bear deuterated porphyrin phenyl groups (C, D = C_6D_5) or that are deuterated at the carbene substituent (Ar = *p*-C_6D_4Cl). With these deuterated derivatives further assignments of resonances to functional groups are possible.

Figure 3 shows an expansion of the crowded region from +14 to −1 ppm for several substituted forms of **2**. Trace A shows the spectrum of **2** (X = I; C, D = *p*-$C_6H_4CH_3$). The two resonances 3.3 and 4.7 ppm are readily assigned to the two *p*-methyl groups on rings C and D because of their relative intensity and their absence in the spectrum shown in Figure 2. This also allows assignment of the *p*-phenyl resonances. The eight resonances in the region 13–7 ppm of trace A have been assigned to the phenyl groups C and D. Notice that they are absent from the spectrum of porphyrin-phenyl-deuterated **2** (X = I; C, D = C_6D_5) shown in trace B of Figure 3. These resonances are divided into two sets; the broader group of four is assigned to the ortho protons, which are closer to the paramagnetic iron center, while the group of four narrow resonances is assigned to the more distant meta protons. Trace C shows the spectrum of the carbene-phenyl-deuterated derivative **2** (X = I; C, D = *p*-C_6H_5; Ar = *p*-C_6D_4Cl). The data allow the four equally intense resonances at 3.1, 1.7, −0.2, and −7.4 ppm (seen in Figure 2) to be assigned to the ortho and meta protons of rings A and B of the inserted carbene. The presence of four equally intense resonances for these eight protons suggests

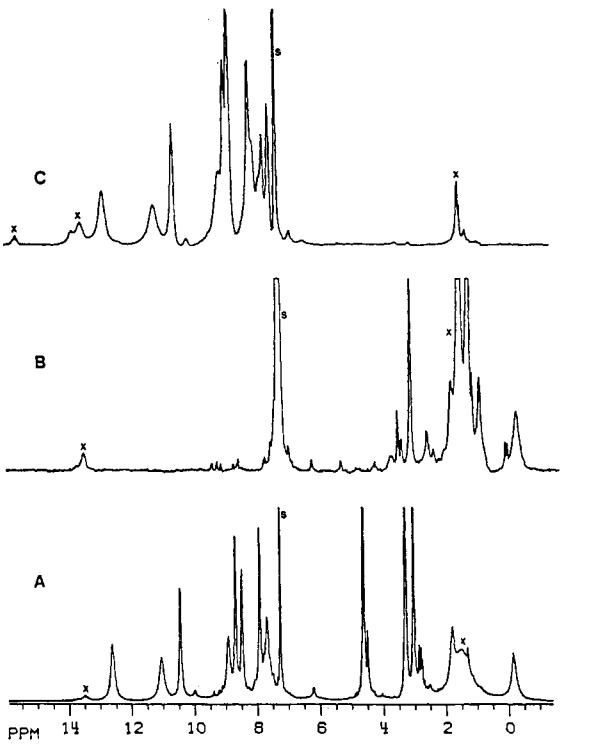

Figure 3. 200-MHz ^{1}H NMR spectra of **2** (chloroform-*d*, 22 °C): (A) X = I, C, D = *p*-$C_6H_4CH_3$, Ar = *p*-C_6H_4Cl; (B) X = I, C, D = *p*-C_6D_5, Ar = *p*-C_6H_4Cl; (C) X = I, C, D = *p*-C_6H_5, Ar = *p*-C_6D_4Cl.

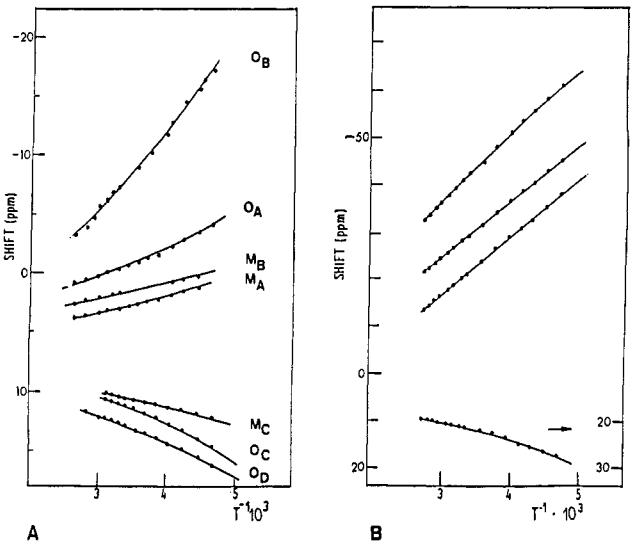

Figure 4. Curie plots of (A) phenyl and (B) pyrrole protons for **2** (X = I; C, D = *p*-C_6H_5; Ar = *p*-C_6H_4Cl) in chloroform-*d* solution.

that ring A does not retain its crystallographic orientation but that either A is free to rotate or it assumes a time-averaged position that is symmetrical with respect to the plane of Fe, Cl, and the carbene carbon.

Curie plots for the resonances that are clearly resolved are shown in Figure 4. Part A shows resonances due to the phenyl rings while part B shows the four pyrrole resonances. It is apparent that there is considerable curvature to these plots, which in general do not extrapolate to the diamagnetic positions expected for such a species.[11,12]

Chemical shift data for **2** with four axial ligands (X^- = Cl^-, Br^-, I^-, N_3^-) are recorded in Table I along with selected line width data. The line widths increase in the order $I^- < Br^- < N_3^- < Cl^-$.

(12) Jesson, J. P. In "NMR of Paramagnetic Molecules"; La Mar, G. N., Horrocks, W. D., Jr.; Holm, R. H., Eds.; Academic Press: New York, 1973; pp 1–52.

Table I. Proton NMR Data for **2** (C, D = p-C_6H_5; Ar = p-C_6D_4Cl)[a]

proton	X⁻			
	I^-[c]	Br^-	Cl^-	N_3^-
pyrrole	21.5 (80.4)[d]	24.2 (85)	25.7 (185)	26.5 (168)
	−21.2 (124.2)	−20.6	−19.7	−19.9
	−29.3 (123)	−25.9	−23.9	−21.5
	−42.3 (138.3)	−41.1	−40.5	−40.4
O_C	11.1 (80.2)	10.3	9.5	9.9
$O_{C'}$	7.8 (50.8)	*b*	*b*	*b*
O_D	12.7 (61.5)	11.3	10.3	10.1
$O_{D'}$	9.0 (59.4)	8.0	8	8.9
M_C	10.5 (12.4)	10.3	10.2	10.7
$M_{C'}$	8.7 (9.1)	8.1	8.1	8.4
M_D	8.8 (10.5)	8.4	8.2	8.2
$M_{D'}$	8.0 (12.0)	7.1	7.9	7.9
para C, D	8.7 (49.6)		8.1	6.9
(p-CH_3)	7.7 (3.2)		6.8	6.1
O_A	−0.2 (101.7)	−0.2	0	*b*
M_A	3.1	2.7	2.6	2.7
O_B	−7.4 (1030)	*b*	*b*	*b*
M_B	1.7 (83.3)	3.6	4.9	4.9

[a] In ppm from Me_4Si with line widths (Hz) in parentheses, T = 298 K, chloroform-d solution. [b] Not visible. [c] Line width data given for −45 °C in dichloromethane-d_2. [d] Line width at 25 °C in chloroform-d 40 Hz.

The trend in line widths, except for the reversal of chloride and azide, parallels that seen in high-spin, five-coordinate iron(III) porphyrin complexes.[13] Because of this trend it has been expeditious to examine preferentially the data for iodide complexes since these have the narrowest and consequently the best resolved resonances. In particular, the broad reonance at −7.5 ppm in Figure 2 due to the O_A protons is not readily observed for the other choices of X. Both the curvature of the Curie plots in Figure 4 and the anion dependence of line width are a result of significant zero-field splitting in these species. The ESR spectrum of **2** has been successfully analyzed by assuming a significant zero-field splitting.[5]

Further Assignments through Temperature Dependence of the Spectrum. The two ortho and meta protons on each of rings C and D are inequivalent since the porphyrin plane bears different substituents on opposite sides and rotation about the meso-carbon–phenyl bond is restricted. However, the onset of rotation about this bond will cause exchange of these positions.[14] Thus pairwise broadening of resonances belonging to rings C and D are expected. Since rings C and D differ, it is anticipated that there will be a slight difference in the rate of phenyl ring rotation for each ring type.

The temperature dependence of the spectrum of **2** (X = I; C, D = $C_6H_4CH_3$) is recorded in Figure 5. Trace A shows the region of the ortho and meta phenyl resonances for a sample in dichloromethane where all resonances are well resolved. Traces B–D show the effect of warming the sample in chloroform solution. Consider first the four narrow meta resonances. When the solution is warmed, the peaks labeled M_C and $M_{C'}$ can be assigned to protons residing on a common phenyl ring and, likewise, peaks M_D and $M_{D'}$ are assigned to the meta protons on the other two phenyl rings. Notice that the peaks labeled M_D and $M_{D'}$ show signs of equivalent broadening at the highest temperature. A similar situation pertains for the ortho resonances. The resonances O_D and $O_{D'}$, which have similar widths, broaden only slightly on warming relative to resonance O_C, which broadens considerably. Unfortunately, the region around resonance $O_{C'}$ cannot be adequately monitored during this transformation. Some decomposition accompanies warming, and this produces debris that causes the growth of a resonance in the 7–8 ppm region. However, the parallel behavior of O_D and $O_{D'}$ dictates that they are paired while the more rapidly broadening resonance O_C must be then paired with $O_{C'}$.

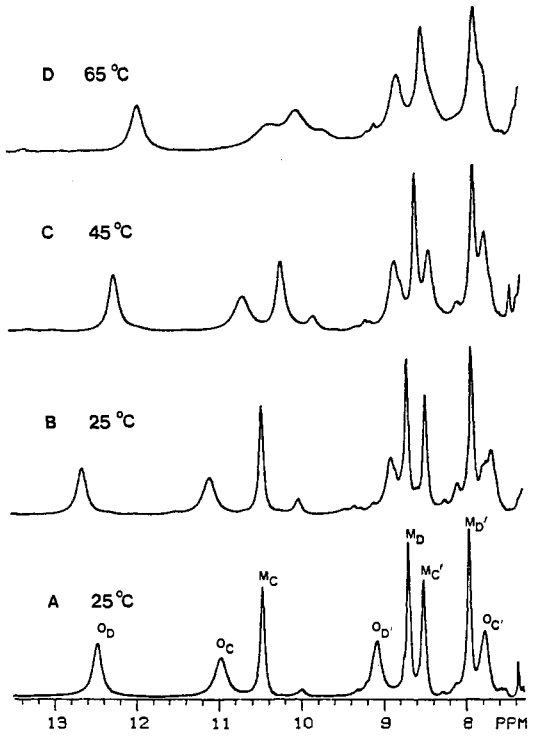

Figure 5. Temperature-dependent 200-MHz NMR spectra of **2** (X = I; C, D = p-$C_6H_4CH_3$) in (A) dichloromethane at 25 °C and in chloroform solution at (B) 25 °C, (C) 45 °C, and (D) 65 °C.

At this stage, however, we cannot yet assign the protons to specific rings (although the labeling scheme does and we will make a connection). That assignment must await the line width analysis, which appears in the following section. However, it is possible now to assign ortho and meta protons to common pairs of phenyl rings. Those peaks that show the onset of differential broadening at lower temperatures must belong to the pair of phenyl rings that are able to rotate more readily. Consequently, peaks labeled M_C, $M_{C'}$, and O_C (and by inference $O_{C'}$) must all belong to one pair of equivalent phenyl rings. This leaves M_D, $M_{D'}$, O_D, and $O_{D'}$ assigned to the other pair of equivalent rings.

Line Width Analysis. For protons that experience negligible contact interaction, the dominant relaxation mechanism is due to the iron dipole, which leads to relative line width proportional to r^{-6}, where r is the iron–proton distance.[15] Values of r have been taken from the X-ray structural data.[9] Qualitatively this allows certain assignments to be made. We have already assigned the ortho and meta porphyrin phenyl resonances on the basis of their relative line widths. Considering only the ortho resonances, the broad resonance O_C and the narrow resonance $O_{C'}$ have been already paired. Now these can be assigned to ortho protons on ring C because this ring has one proton that is the closest of all ortho protons to the iron and one proton that is the furthest of the ortho protons from the iron. The other two ortho protons, which have very similar line widths, are assigned to phenyl ring D, which has comparable r and r^{-6} values for both of its protons. The previously obtained connection between ortho and meta protons allows then the meta protons to be assigned to specific pairs of rings. For the carbene rings A and B, the ortho protons of ring B are expected to be closest to iron and these are assigned to the broad peak at −7.5 ppm of Figure 1. The relative line widths expected for carbene phenyls A and B are $O_B > O_A > M_B > M_A$, and the resonances have been assigned accordingly. With these assignments the plot of line width vs. r^{-6} shown in Figure 6 has been made. The agreement in most cases is quite satisfactory, particularly when it is realized that the r values have been obtained for the chloro complex while the most extensive and best resolved

(13) La Mar, G. N.; Walker, F. A. *J. Am. Chem. Soc.* **1973**, *95*, 6950.
(14) Eaton, S. S.; Fishwild, D. M.; Eaton, G. R. *Inorg. Chem.* **1978**, *17*, 1542 and references therein.
(15) Swift, T. J. In "NMR of Paramagnetic Molecules"; La Mar, G. N., Horrocks, W. D., Jr.; Holm, R. H., Eds.; Academic Press: New York, 1973; pp 53–83.

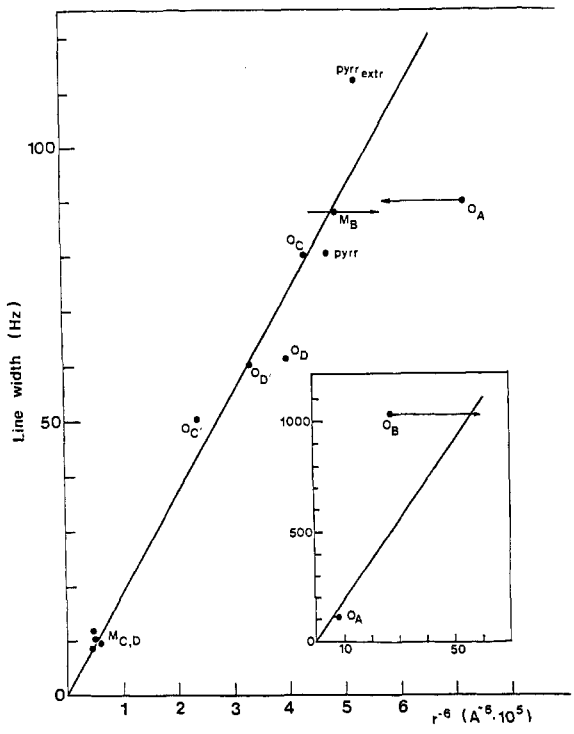

Figure 6. Plot of line width vs. r^{-6} for **2** (X = I; C, D = *p*-$C_6H_4CH_3$; Ar = *p*-C_6H_4Cl) in dichloromethane-d_2 at −45 °C. The peak pyrr extr is the extrapolated pyrrole resonance from pyrroles 2, 3, and 4 after correction for the chemical shift differences.

line width data (and the data we have used) relate to the iodo complex. Consequently, some degree of error is expected.

The signals whose line widths deviate the most from the plot of line width vs. r^{-6} are the carbene phenyl protons. This is due to assuming a rigid orientation with ring A in the twofold plane and ring B perpendicular to it. If, on the other hand, 30° tilts are assumed for both rings which are symmetrically time averaged, the respective computed r^{-6} values move in the direction and by an amount shown by the respective arrows for these signals as in Figure 6. The much closer fit of the relative line widths to r^{-6} thus suggests such motion for the carbene phenyls.

The importance of scalar relaxation[16] or local dipolar relaxation by delocalized spin density is evidenced by the variable line width for the pyrrole-H signals, even though the values of r for three of them are the same in the crystal.

Spectral Patterns for Octaethylporphyrin and Protoporphyrin IX Complexes. In order to establish shift patterns that are relevant to the problem of detecting structure **1** in proteins, the ^1H NMR spectra of analogues **3** and **4** derived from octaethylporphyrin and protoporphyrin IX dimethyl ester, respectively, were obtained. The results are shown in Figure 7.

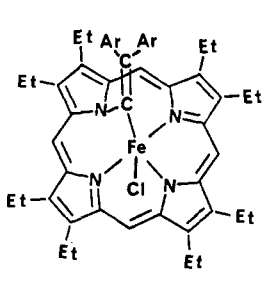

3

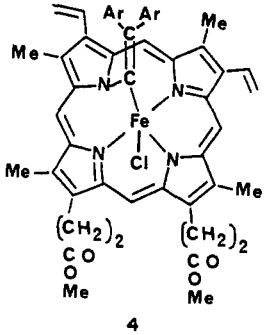

4

Trace A shows the spectrum of **3**. Eight methylene resonances of equal intensity are apparent in the downfield region. These

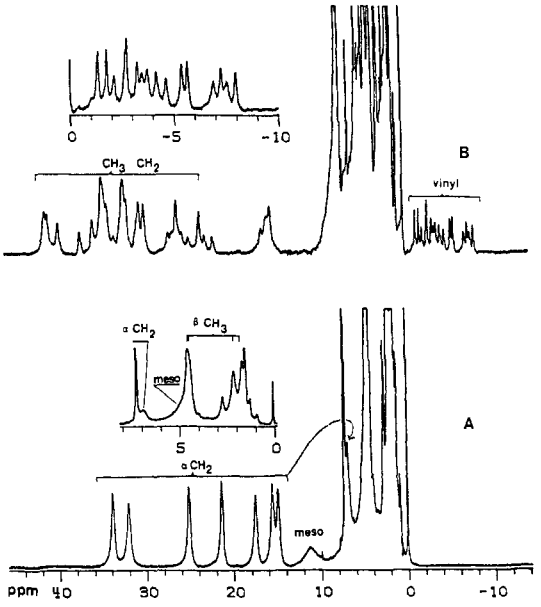

Figure 7. Proton NMR spectra of (A) the octaethylporphyrin complex **3** at 23 °C and 360 MHz in chloroform-*d* at 25 °C and (B) the protoporphyrin IX dimethyl ester complex **4** (mixture of isomers).

arise because there are four distinct methyl groups present in **3** and the protons in each methylene are diastereotopic. One meso resonance, identified by relative intensity and line width, is clearly visible at 11.5 ppm, while the other is hidden under the methyl resonance near 5 ppm. The insert shows the positions of the methyl resonances. The resonances of the *p*-chlorophenyl substituents are not fully resolved in these spectra, although some are detectable in the 2–0 ppm region.

Trace B shows the spectrum of **4**. Four isomers are expected since there are four unique pyrrole rings to which the carbene moiety could migrate. Only one of these is depicted in **4**. The spectrum in trace B shows a series of resonances in the downfield region which are assigned to the porphyrin methyls and methylenes on the basis of comparison with the methylene positions in the spectrum of **3**. In the region from 0 to −10 ppm there is a series of 15 resolved resonances, which are assigned to the β-vinyl protons on the basis of their absence in the spectrum of the analogous derivative of deuterohemin[4] and similarity in shift patterns to those of other ferric model complexes.[11] Since 16 resonances are expected if all four isomers are present, the spectra indicate that all four isomers exist within the sample.

Analysis of Hyperfine Shifts in Terms of Magnetic Properties and Electron Structure. The observed hyperfine shifts are the sum of the scalar or contact contribution, which reflects the mode of spin delocalization, and any dipolar shift due to magnetic anisotopy of the iron. The dipolar shift is given by[12] $\Delta H/H = -^2/_3[\chi_{zz} - {}^1/_2\chi_{xx} - 1/2\chi_{yy})](3\cos^2\theta - 1)\, r^{-3} + 1/2(\chi_{xx} - \chi_{yy})\sin^2\theta\cos 2\Omega$, where θ and Ω are the polar and azimuthal angles which determine the direction of r in the Cartesian coordinate system.

The general pattern of shifts for the meso phenyl groups (all in one direction and all attenuating with distance from the iron) and the relative direction of the axial carbene phenyl rings, A, B (upfield), and the meso phenyl group (all downfield) are strongly indicative of dominant axial dipolar interaction, i.e. $\chi_{xx} \sim \chi_{yy}$, so that the observed relative shifts should parallel the computed relative values of the geometric factor $(3\cos^2\theta - 1)r^{-3}$. Such a plot using the X-ray data is illustrated in Figure 2. The correlation is quite good, and deviations are significant only for the carbene A and B phenyl rings. Here, again, these data points move closer to the line when large oscillatory motion of the carbene phenyl rings is taken into account. However, since these rings are close to the magic angle ($\theta = 54°$), large discrepancies can also arise from only small variations in coordinates. Thus it does not appear fruitful to search for a more quantitative fit. The semiquantitative correlation in Figure 8, however, does demonstrate that the complex exhibits primarily axial anisotopy with negative zero-field

(16) Unger, S. W.; Jue, T.; La Mar, G. N. *J. Magn. Reson.* **1985**, *61*, 448.

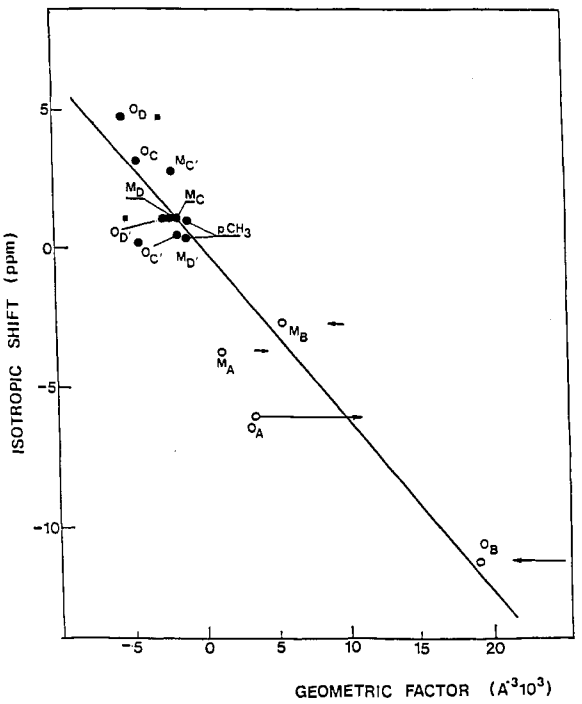

Figure 8. Isotropic dipolar shift vs. geometric factor for **2** (X = I; C, D = p-$C_6H_4CH_3$; Ar = p-C_6H_4Cl) in chloroform-d at 25 °C.

splitting constant, D[13], in spite of the large in-plane distortion caused by the carbene insertion into one Fe–N bond.

The significantly smaller line width of pyrrole-H at 20 ppm as well as its unique shift direction argues for its assignment to the unique pyrrole 1 between the C phenyl rings. With use of the dipolar shifts for meso phenyl protons and the relative axial geometric factors for the phenyl proton and the four pyrrole-H's, a downfield dipolar shift of 5 ppm is calculated[11] for each pyrrole-H. Thus, the pyrrole-H contact shifts are large and upfield for the three "normal" pyrroles. The spectra of **3** and **4** show that all pyrrole methyl and methylene contact shifts are downfield. Thus the contact shift pattern for the three "normal" pyrrole protons reflects extensive spin delocalization into a π MO,[17] as found for other $S = {}^3/_2$ ferric complexes.[18] The dominance of the π-spin transfer mechanism can also be taken as direct evidence that $d_{x^2-y^2}$ is not populated. Thus, of the two alternate ground states $(d_{xy})^2(d_{xz})^1(d_{yz})^1(d_{x^2-y^2})^1$ and $(d_{xy})^2(d_{xz})^1(d_{yz})^1(d_{z^2})^1$, the NMR data support only the latter configuration.

The variation in line width, δ, as a function of the halide ligand X is parallel to that observed previously for high-spin ferric complexes[13,19] and originates from an electron spin relaxation modulated by a large axial zero-field splitting, D, i.e. $\delta \propto D^{-2}$. Thus the zero-field splitting is largest for the iodide and smallest for Cl^-. This ordering dictates that D is negative.[13]

The influence of the large zero-field splitting is also apparent in the temperature dependence of the hyperfine shifts. The phenyl ring signals all exhibit significant curvature in the Curie plot (Figure 4) as predicted by[12,18] the T^{-2} contribution to the shift from zero-field splitting. The pyrrole-H shifts (particularly for the three "normal" pyrroles) exhibit only a small dipolar contribution to their shift and hence exhibit more linear plots as expected for contact shifts.

Thus we conclude that the ^{1}H NMR paramagnetic shift and line width data for these complexes are consistent with the low symmetry produced by the carbene insertion into a Fe–N bond. The complexes exhibit axial magnetic anisotropy dominated by a negative zero-field splitting and iron–pyrrole π bonding similar to that in other ferric $S = {}^3/_2$ systems.

Experimental Section

Materials. Tetraphenylporphyrin (TPP), tetra-p-tolylporphyrin (TpTP), and phenyl-deuterated tetraphenylporphyrin (TPP-d_{20}) (from benzaldehyde-d_5) were prepared as described previously.[20] Octaethylporphyrin (OEP) and protoporphyrin IX dimethyl ester (PPDME) were purchased from Man-Win Chemical Co. All the corresponding iron(III) chloro complexes were prepared and purified as described in the literature.[21] 2,2-Bis(p-chlorophenyl)-1,1,1-trichloroethane (DDT) was purchased from Aldrich Chemical Co. Chlorobenzene-d_5 was supplied by Isotopische Reinheit. Chloral hydrate was obtained from Sigma Chemical Co. Iron powder was obtained from Mallinckrodt Chemical Works. DDT-d_8 was prepared from chloral hydrate and chlorobenzene-d_5 in concentrated sulfuric acid by a literature procedure.[22]

Synthesis of Vinylidene Carbene Complexes of Iron(II) Porphyrins. The procedure published by Mansuy et al.[5] was modified as follows: 300 mg of (P)FeCl and excess iron powder (3 g) were added to a 100-mL three-neck round-bottom flask equipped with a 2 cm long magnetic stirrer. About 1.4 equiv (210 mg) of solid DDT was kept at a side arm. The whole system was flushed with argon through a gas inlet adaptor. The third neck, which was sealed with a septum cap, could be used as a gas outlet through a syringe. About 60 mL of CH_2Cl_2/CH_3OH (9:1) solvent mixture was purged with argon for 20 min and then added to the flask. The porphyrin solution was stirred vigrously until all the iron(III) porphyrin had been reduced. This occurred after about 30 min, when the solution turned red. Then DDT was added in small portions over a 3-h period. The reaction mixture was stirred for another 0.5 h. The excess iron powder was removed by filtration, and the solution was washed with 2 × 30 mL of water containing sodium dithionite (5 g/100 mL). The solvent was then removed by evaporation, and the residue was recrystallized from CH_2Cl_2/CH_3OH. The product **1** was identified by comparison of the electronic and ^{1}H NMR spectra with those reported by Mansuy et al.[5] The yield for this reaction depends very much on the reduction and can vary from 50% to 80%.

One-Electron Oxidation of Iron(II) Porphyrin Vinylidene Carbene Complexes. There are two different ways to accomplish the oxidation: (1) About 1 equiv of oxidizing agent (0.1 M $FeCl_3$ in CH_3CN to give the chloro complex or 0.1 M I_2 in C_6H_6 to give the iodo complex) was added progressively within 1 h to a 1 mM benzene solution of 300 mg of purified **1**. (2) The filtrate from the original separation above before washing with aqueous dithionite was stirred under air for 10 min. Under these conditions ferrous ions resulting from reduction were oxidized to the ferric form by O_2 and these served as oxidizing agent. After oxidation, the solvent was evaporated, and the residue was purified by chromatography on a column (3 × 25 cm) of silica gel with elution by benzene/acetone. Recrystallization from acetone/hexane gave yields of **2** always higher than 80%. This procedure can be scaled down to work with 5 mg of porphyrin.

Ligand Exchange of the Anion of (P)Fe(VC)Cl. Metathesis was (X = Cl) accomplished by vigorously stirring a 1 mM benzene solution of **2** with a saturated aqueous solution of the sodium salt of the desired anion for about 2 h. The benzene solution was separated from the mixture by means of a pipet, and the solution was evaporated to dryness using a rotary evaporator. The resulting solid was then redissolved in acetone, filtered, and reprecipitated by the addition of hexane. A series of **2** with X = Cl, Br, I, and N_3 has been made this way. Anal. Calcd for **1** (X = I; C, D = C_6H_5), $C_{58}H_{36}N_4Cl_2IFe$: C, 66.82; H, 3.48; N, 5.37; Cl, 6.80. Found: C, 67.47; H, 3.56; N, 5.37; Cl, 6.70.

Spectroscopic Measurements. All ^{1}H NMR spectra were recorded at 360 or 200 MHz on a Nicolet NT-360 or NT-200 spectrometer operating in the quadrature mode. Peak positions (in ppm) were referenced to tetramethylsilane. Typical spectra required 300–2000 transients collected over a 4–40-kHz bandwidth with a 10-μs 90° pulse. Solutions used for spectroscopy were ca. 1 mM in iron complex and, because of the decidedly nonplanar shape of the molecules, showed no evidence of aggregation.

Acknowledgment. We thank the National Institutes of Health (Grant No. GM-26226) for support. L.L.-G. was on leave from the Institute of Chemistry, University of Wrocław, Wrocław, Poland.

(17) La Mar, G. N. In "NMR of Paramagnetic Molecules"; La Mar, G. N., Horrocks, W. D., Jr., Holm, R. H., Eds.; Academic Press: New York, 1973; pp 85–126.
(18) Goff, H.; Shimomura, E. *J. Am. Chem. Soc.* **1980**, *102*, 31.
(19) Walker, F. A.; La Mar, G. N. *Ann. N.Y. Acad. Sci.* **1973**, *206*, 328.
(20) Adler, A. D.; Longo, F. R.; Finareli, J. F.; Goldmacher, J.; Assour, J.; Korsakoff, L. *J. Org. Chem.* **1967**, *32*, 476.
(21) Adler, A. D.; Longo, F. R.; Kampas, F.; Kim, J. *J. Inorg. Nucl. Chem.* **1970**, *32*, 2443.
(22) Ginsburg, J. M. *Science (Washington, D.C.)* **1948**, *108*, 339.

Registry No. **2** (C, D = p-C_6H_5; Ar = p-C_6D_4Cl, X = I), 97170-30-4; **2** (C, D = p-C_6H_5; Ar = p-C_6D_4Cl, X = Br), 97170-31-5; **2** (C, D = p-C_6H_5; Ar = p-C_6D_4Cl, X = Cl), 97170-32-6; **2** (C, D = p-C_6H_5; Ar = p-C_6D_4Cl, X = N_3), 97170-33-7; **2** (C, D = p-$C_6H_4CH_3$; Ar = p-C_6H_4Cl, X = I), 97170-34-8; **2** (C, D = p-C_6D_5; Ar = p-C_6H_4Cl, X = I), 97170-35-9; **2** (C, D = p-C_6H_5; Ar = p-C_6H_4Cl, X = I), 97170-36-0; **3**, 97149-92-3; **4** (isomer 1), 97149-93-4; **4** (isomer 2), 97149-94-5; **4** (isomer 3), 97170-37-1; **4** (isomer 4), 97170-38-2.

Contribution from the Departments of Chemistry and Physics,
The Pennsylvania State University, University Park, Pennsylvania 16802

Synthesis, Oxygen-Binding Behavior, and Mössbauer Spectroscopy of Covalently Bound Polyphosphazene–Heme Complexes[1]

HARRY R. ALLCOCK,*† THOMAS X. NEENAN,† and BRIAN BOSO‡

Received January 15, 1985

The water-soluble poly(aminophosphazene) $[NP(NHCH_3)_x(NCH_3CH_2CH_2CH_2NH_2)_y]_n$ has been investigated as a polymeric carrier molecule for the covalent attachment of (a) a modified picket fence hemin (**3**) and (b) protohemin chloride 3-(1-imidazolyl)propylamide (**4**). Reduction of the polymer-bound species with dithionite in DMF/H_2O 9:1 or H_2O/ethylene glycol 1:1 yielded the corresponding heme complexes. The oxygenation behavior of these species was examined at −30 °C and at room temperature by electronic absorption spectroscopy. Polymer-bound **4** gave a stable O_2 adduct at −30 °C in DMF/H_2O but was oxidized in ethylene glycol/H_2O. Polymer-bound **3** gave a stable O_2 adduct in DMF/H_2O or ethylene glycol/H_2O only in the presence of excess axial base. Solid films of the two polymer-bound hemes were inert to oxygen for periods of weeks but did react with carbon monoxide to yield carbonmonoxy derivatives. The oxygenation behavior of the cross-linked films swollen with solvent showed a closer resemblance to that of the solution-state systems than to that of the solid state. Dc polarography was performed on the two polymeric hemins, and cathodic shifts relative to the free hemins of >100 mV were seen for both species. Iron-57-labeled derivatives of hemin **3** were prepared, and the oxygenation behavior of the polymer-bound iron-57-labeled species was examined by Mössbauer spectroscopy. The small molecule species $N_3P_3(OPh)_5[N(CH_3)CH_2CH_2CH_2NH_2]$ was synthesized as a model for the high polymer, and the corresponding derivatives with **3** and **4** were prepared.

Polymer-bound metallo compounds are of interest for uses in catalysis,[2] membrane technology,[3] electrode modification,[4] and bioinorganic model chemistry.[5] In this present work, we have explored the use of an inorganic–organic polymer system, based on a polyphosphazene backbone, as a carrier for metalloporphyrins. In an earlier study[6] we examined the influence of a water-soluble aminophosphazene polymer as a *coordination* carrier for heme or hemin.[6] Here, we consider the effect of *covalent* bonding between the water-soluble carrier macromolecule and two metalloporphyrins on the oxygen-binding and electrolytic characteristics of the systems. We were particularly interested in comparisons between the oxidation or oxygenation behavior of these species in the solid state and in solution.

The field of polymer-bound or silica-immobilized metalloporphyrin chemistry is an active and, in some respects, controversial research area. Its development can be traced to the well-known anomaly that hemoglobin or myoglobin bind dioxygen reversibly but simple ferrous compounds are irreversibly oxidized in the presence of oxygen and water. Free heme molecules are also sensitive to Fe(II) → Fe(III) oxidation. Hence, the proteinoid macromolecular "carrier" in hemoglobin or myoglobin is assumed to retard oxidation and permit reversible oxygenation. Various specific roles have been ascribed to the protein molecules, including a physical separation of the heme units to prevent μ-oxo dimer formation, the generation of a hydrophobic pocket around the metalloporphyrin to retard oxidative electron transfer from iron to oxygen, coordination of heme to only one imidazole (histidine) unit to leave the sixth coordination site essentially free for oxygen binding, and the formation of an environment of low acidity, which retards oxidation.

Thus, various model systems have been devised to test each of these influences.[8] The hydrophobic environment and physical separation hypotheses have been tested by Collman[9] and Baldwin[10] with their respective "picket fence" and capped porphyrin species. The requirement for mono(base) coordination was examined by Traylor[11] through the synthesis and flash photolysis of modified hemes with pendent, covalently attached imidazole. The ideas of a physical separation of metalloporphyrin units and the need for a hydrophobic environment were also tested by Wang[12] who embedded a heme ester in a solid, hydrophobic polystyrene matrix and detected reversible oxygen binding. Collman[14] has investigated

† Department of Chemistry.
‡ Department of Physics.

(1) For other papers on the use of polyphosphazenes as carrier molecules for inorganic, organic bioactive, or catalytic species, see: Allcock, H. R.; Allen, R. W.; O'Brien, J. P. *J. Am. Chem. Soc.* **1977**, *99*, 3984. Allen, R. W.; O'Brien, J. P.; Allcock, H. R. *J. Am. Chem. Soc.* **1977**, *99*, 3987. Allcock, H. R.; Fuller, T. J. *Macromolecules* **1980**, *13*, 1338. Allcock, H. R.; Austin, P. E. *Macromolecules* **1981**, *14*, 1616. Allcock, H. R.; Austin, P. E.; Neenan, T. X. *Macromolecules* **1982**, *15*, 693. Neenan, T. X.; Allcock, H. R. *Biomaterials* **1982**, *3*, 2, 78. Allcock, H. R.; Lavin, K. D.; Tollefson, N. M.; Evans, T. L. *Organometallics* **1983**, *2*, 267. Allcock, H. R.; Austin, P. E. *Macromolecules* **1983**, *16*, 1401.
(2) (a) Grubbs, R. H. *CHEMTECH* **1977**, *7*, 512. (b) Sekiya, A.; Stille, J. K. *J. Am. Chem. Soc.* **1981**, *103*, 5096.
(3) Lonsdale, H. K. *J. Membr. Sci.* **1982**, *10*, 81.
(4) (a) Calvert, J. M.; Meyer, T. J. *J. Am. Chem. Soc.* **1981**, *103*, 27. (b) Buttry, D. A.; Anson, F. C. *J. Am. Chem. Soc.* **1982**, *104*, 4824.
(5) (a) Tazuke, S.; Tomono, H.; Kitamura, N.; Sato, K.; Hayoshi, N. *Chem. Lett.* **1979**, *85*. (b) Tsuchida, E.; Hasegawa, E.; Honda, K. *Biochim. Biophys. Acta* **1976**, *427*, 520.
(6) Allcock, H. R.; Greigger, P. P.; Gardner, J. E.; Schmutz, J. L. *J. Am. Chem. Soc.* **1979**, *101*, 606.
(7) (a) Perutz, M. F. *Nature (London)* **1970**, *228*, 726. (b) Perutz, M. F.; Heidner, E. J.; Ladner, R. C. *J. Mol. Biol.* **1976**, *104*, 707. (c) Jones, R. D.; Summerville, D. A.; Basolo, F. *Chem. Rev.* **1979**, *79*, 139.
(8) For reviews of the model compound approach to iron porphyrin chemistry see: (a) Collman, J. P. *Acc. Chem. Res.* **1977**, *10*, 265. (b) Traylor, T. G. *Acc. Chem. Res.* **1981**, *14*, 102.
(9) (a) Collman, J. P.; Gagne, R. R.; Reed, C. A.; Halbert, T. R.; Lang, G. Robinson, W. T. *J. Am. Chem. Soc.* **1975**, *97*, 1427. (b) Collman, J. P.; Gagne, R. R.; Halbert, T. R.; Marchon, J.-R.; Reed, C. A. *J. Am. Chem. Soc.* **1973**, *95*, 7868.
(10) (a) Baldwin, J. E.; Almog, J.; Huff, J. *J. Am. Chem. Soc.* **1975**, *97*, 226. (b) Baldwin, J. E.; Almog, J.; Dyer, R. L.; Peters, M. *J. Am. Chem. Soc.* **1975**, *97*, 227.
(11) (a) Chang, C. K.; Traylor, T. G. *Proc. Natl. Acad. Sci. U.S.A.* **1973**, *70*, 2647. (b) Chang, C. K.; Traylor, T. G. *J. Am. Chem. Soc.* **1973**, *95*, 5810. (c) Traylor, T. G.; Chang, C. K.; Geibel, J.; Berzinis, A.; Mincey, T.; Cannon, J. *J. Am. Chem. Soc.* **1979**, *101*, 6716.
(12) Wang, J. H. *J. Am. Chem. Soc.* **1958**, *80*, 3168.
(13) Leal, O.; Anderson, D. L.; Bowman, R. G.; Basolo, F.; Burwell, R. L., Jr. *J. Am. Chem. Soc.* **1975**, *97*, 5127.

0020-1669/85/1324-2656$01.50/0